GLOBAL BIOGEOCHEMICAL CYCLES, VOL. 14, NO. 2, PAGES 559-572, JUNE 2000

On the origin and timing of rapid changes in atmospheric methane during the last glacial period

Edward J. Brook,[1] Susan Harder,[1] Jeff Severinghaus,[2] Eric J. Steig,[3] and Cara M. Sucher[4,5]

Abstract. We present high resolution records of atmospheric methane from the GISP2 (Greenland Ice Sheet Project 2) ice core for four rapid climate transitions that occurred during the past 50 ka: the end of the Younger Dryas at 11.8 ka, the beginning of the Bølling-Allerød period at 14.8 ka, the beginning of interstadial 8 at 38.2 ka, and the beginning of interstadial 12 at 45.5 ka. During these events, atmospheric methane concentrations increased by 200-300 ppb over time periods of 100-300 years, significantly more slowly than associated temperature and snow accumulation changes recorded in the ice core record. We suggest that the slower rise in methane concentration may reflect the timescale of terrestrial ecosystem response to rapid climate change. We find no evidence for rapid, massive methane emissions that might be associated with large-scale decomposition of methane hydrates in sediments. With additional results from the Taylor Dome Ice Core (Antarctica) we also reconstruct changes in the interpolar methane gradient (an indicator of the geographical distribution of methane sources) associated with some of the rapid changes in atmospheric methane. The results indicate that the rise in methane at the beginning of the Bølling-Allerød period and the later rise at the end of the Younger Dryas were driven by increases in both tropical and boreal methane sources. During the Younger Dryas (a 1.3 ka cold period during the last deglaciation) the relative contribution from boreal sources was reduced relative to the early and middle Holocene periods.

1. Introduction

Studies of ice cores from Greenland and Antarctica reveal that significant changes in atmospheric methane concentration occurred with a range of periods over the past 400,000+ years [*Rasmussen and Khalil*, 1984; *Khalil and Rasmussen*, 1987; *Raynaud et al.*, 1988; *Stauffer et al.*, 1988; *Chappellaz et al.*, 1990, 1993a, 1997; *Etheridge et al.*, 1992; *Jouzel et al., 1993*; *Blunier et al.*, 1993, 1995; *Brook et al.*, 1996a, 1999; *Petit et al.*, 1999]. Wetlands are the major natural methane source [*Fung et al.*, 1991; *Chappellaz et al.*, 1993b; *Hein et al.*, 1997], and research in modern wetlands suggests that methane emissions depend on temperature, hydrologic balance, and possibly net ecosystem production [*Whiting and Chanton*, 1993; *Bubier and Moore*, 1994; *Schlesinger*, 1996]. Warm, wet, and highly productive conditions are associated with higher methane emissions. As a result, ice core methane records have been interpreted as indicators of terrestrial climatic conditions on a variety of timescales.

Long records from the Vostok ice core indicate that atmospheric methane concentrations varied on timescales associated with orbital forcing. A 20,000 year periodicity in the Vostok record was attributed to the effects of solar insolation variations on the tropical monsoon cycle [*Chappellaz et al.*, 1990; *Petit-Maire et al.*, 1991], or alternatively, to temperature and precipitation variations in high latitude wetland regions [*Crowley*, 1991]. More recently, higher-resolution records have become available from cores through the rapidly accumulating Greenland Ice Sheet. Methane records from the Greenland Ice Sheet Project 2 (GISP2) and Greenland Ice Core Program (GRIP) ice cores support the general patterns revealed at Vostok [*Chappellaz et al.*, 1993a; *Brook et al.*, 1996a]. They also reveal that atmospheric methane levels varied significantly on millennial timescales during the last glacial period. The millennial variations were coeval with millennial-scale warmings and coolings (interstadial events) inferred from oxygen isotope records from central Greenland ice cores, proxies for surface temperature [*Johnsen et al.*, 1993; *Grootes et al.*, 1993]. The ice core methane record therefore indicates a close relationship between interstadial climate and changes in terrestrial methane emissions [*Chappellaz et al.*, 1993a]. This conclusion augments a large body of evidence suggesting a correlation between rapid climate change in Greenland ice core records and terrestrial climate change in a variety of locations around the world [e.g., *Grimm et al.*, 1993; *Broecker et al.*, 1998; *Gasse and Van Campo*; 1998, *Grigg and Whitlock*, 1988; *Allen et al.*, 1999].

Gaps in our understanding of millennial-scale shifts in methane concentration include incomplete knowledge of (1) the detailed timing and magnitude of the rapid concentration changes, (2) the possible role of massive releases of clathrate-bound methane from marine sediments and permafrost, and (3) the methane source locations and how they changed with time. In this paper we examine these issues using methane records covering the past 50,000 years from two ice cores, the GISP2

[1]Department of Geology, Washington State University, Vancouver.
[2]Scripps Institution of Oceanography, University of California, San Diego, La Jolla.
[3]Department of Earth and Environmental Science, University of Pennsylvania, Philadelphia.
[4]Graduate School of Oceanography, University of Rhode Island, Narragansett, Rhode Island.
[5]Now at NOAA Office of Global Programs,Silver Spring, Maryland.

Paper number 1999GB001182.
0886-6236/00/1999GB001182$12.00

core from central Greenland and the Taylor Dome core from the Ross Sea sector of Antarctica. We use the results to constrain the rate and magnitude of methane concentration change associated with rapid climate shifts during the last glacial period and deglaciation. We also determine the interpolar methane gradient, a possible proxy for the geographical distribution of methane sources [*Rasmussen and Khalil, 1984*], at selected time intervals, and examine the implications of changes in the gradient.

2. Samples and Analytical Procedures

2.1. Ice Core Samples

The GISP2 ice core was recovered in 1993 at 72°36'N, 38°30'W in central Greenland. We have extended our original GISP2 data set [*Brook et al.*, 1996a] by analyzing samples from 129 additional depths in the upper 2438 m, which represents the past 50 ka. We focused on abrupt transitions in the record, including the termination of the Younger Dryas period at ~11.8 ka, the beginning of the Bølling-Allerød period at ~14.5 ka, and the onsets of interstadials 8 and 12, rapid warming events that occurred at ~ 38.2 and 45.5 ka in the GISP2 isotope record. The GISP2 methane data set over the 0-50 ka interval now includes 289 sample depths. The Taylor Dome ice core was recovered in 1994 at 77°48'S, 159°53'E on Taylor Dome, a small ice dome in the Ross Sea sector of Antarctica. The Taylor Dome paleoclimate record extends to greater than 130 ka at a depth of 554 m [*Grootes and Steig*, 1994; *Steig*, 1996; *Steig et al.*, 2000] but we focus here on methane measurements of 137 samples in the upper 445 m (0-50 ka), with high resolution measurements over the time intervals listed above. Data are available from the National Oceanic and Atmospheric Administration (NOAA) Geophysical Data Center (http://www.ngdc.noaa.gov/) or from the authors.

2.2. Analytical Methods

Ice samples weighing ~35 g were placed in cubical stainless steel vacuum vessels with volumes of ~ 40 cm^3. The vessels have Nupro SS-4H stainless steel bellows valves and were sealed with gold o-rings. The vessels were attached to a vacuum line with stainless steel Swagelock fittings with Teflon ferrules. They were maintained at -25° to -30°C in an alcohol bath cooled with a cryogenic probe chiller (FTS Systems MFC-100). Ambient air was removed by pumping with a mechanical vacuum pump for 30 min. Ice samples were isolated from the pump and allowed to melt in a warm water bath for 30 minutes. The samples were refrozen by lowering the vessels slowly into a -80°C alcohol bath over a 30 min. time period. This procedure expels the air trapped in the ice into the evacuated vessel headspace. The vessels were attached to a welded stainless steel vacuum line constructed with Nupro SS-4H valves. The line served as the inlet to a Hewlett-Packard Model 5890 Series II gas chromotagraph (GC) equipped with a six-port gas sampling valve, a 10 cm^3 sample loop, a Poropak Q column, and a flame ionization detector. The GC sample loop and vacuum line were evacuated to a pressure of ~ 10^{-3} torr with a mechanical vacuum pump. The headspace gas was introduced to the sample loop, and the pressure in the sample loop was measured with an MKS Model 122A Baratron Capacitance Manometer fixed to the outlet port of the gas sampling valve. The gas extracted from individual ice samples was normally analyzed twice. The loop pressures for the first and second measurements were 40-50 and 15-20 torr, respectively.

Methane concentrations were quantified by measuring peak areas using ELAB (OMS Tech, Miami, Florida) chromatographic software and computer interface. Our working standard was a high-pressure cylinder of synthetic air prepared by Scott-Marin Specialty Gases. This standard has a methane concentration of 962 ± 6 ppb (mean ± 2 times SE, where SE is standard error), determined by comparison to two similar cylinders that were calibrated at the NOAA/Climate Monitoring and Diagnostics Laboratory, which have methane concentrations of 1488±3 ppb and 1824±3 ppb. We calibrated the instrument daily with six to eight injections of the working standard at a range of sample loop pressures between 10 and 60 torr. The average daily precision of these runs of the calibration standard was ± 9 ppb (2 x SE, n=347).

Contamination in our sample processing was evaluated in two ways. First, we ran a total analytical blank, as follows. An ice sample analyzed the previous day was melted and refrozen 3 times in a vacuum vessel. After each refreezing step any remaining air in the vessel was pumped out. The ice sample was removed from the vessel, and the edges were trimmed with the band saw normally used to cut ice samples. The ice cube was then placed in a second vessel, and the ambient air was pumped out while maintaining the vessel at -30°C. The vessel was then cooled to -80°C. One hundred torr of standard air was introduced into the vacuum line and sample vessel, the vessel valve was closed, and the remainder of the line was evacuated. One hundred torr in the sample vessel resulted in a pressure of 40-50 torr in the GC sample loop when the gas was expanded, a value similar to that obtained when analyzing most ice samples. This "blank sample" was then melted and refrozen. We analyzed the air in the headspace and determined the blank as the difference between the expected value of the standard and the measured value. Blanks measured in this way over a 27 month time period had a mean of 16 ± 4 ppb (mean ± 2 x SE, n=63).

In an attempt to locate the source of contamination, we performed an additional blank experiment. After analysis of an ice core sample was completed and while the sample was still frozen, we evacuated the sample container and introduced 100 torr of standard in the line and vessel. The vessels were sealed for 5 min., and the line was evacuated. The gas in the vessels was then analyzed in the normal fashion. This blank test should detect contamination due only to the vacuum line and sample vessel and exclude contamination specifically due to the melting and refreezing step. The mean of blanks performed this way with different sample vessels and samples over a one month period was 3±4 ppb (mean ± 2 x SE, n=20), suggesting that most of the contamination in our procedure is due to the melting and refreezing step. We are not certain if this contamination is due to small vacuum leaks or chemical reactions between the water and the stainless steel vacuum vessel. *Fuchs et al.* [1993] suggested that the compression of stainless steel on stainless steel might produce methane. Our results suggest that the mechanical action of the stainless steel bellows and the contact of the stainless steel stem tip with the valve body are not major sources of contamination in our analyses.

To generate the records presented here we analyzed at least two separate ice samples at each sample depth and analyzed the headspace gas for each twice (averaging the results for the two

injections). If analyses of duplicate ice samples disagreed by more than 5%, a third replicate was analyzed. For 859 duplicate pairs (not all measured for this study) meeting the 5% criteria, analyzed between 1993 and 1997 in the URI laboratory, the average deviation from the mean value was 1.2%. We occasionally also rejected a result if the pressure in the sample loop was significantly lower than usually observed, which we attribute to incomplete melting or gas loss prior to analysis. These analyses generally resulted in anomalously high methane concentrations.

3. Methane Records

3.1. Gas Age and Ice Age Timescales

To compare methane records from different ice cores, a common temporal framework is necessary. The methane records themselves provide one way of creating that framework because the atmospheric mixing time (~1 year) is short enough that interannual variations in methane concentration are essentially synchronous in both hemispheres. The isotopic composition of atmospheric O_2 ($\delta^{18}O_{atm}$) trapped in polar ice can be used in a similar way, because $\delta^{18}O_{atm}$ varied significantly over the past 50,000 years, primarily owing to changes in the $\delta^{18}O$ of seawater [Bender et al., 1994].

Our strategy was to use the GISP2 timescale, determined primarily by counting annual layers for the last 50 ka [*Meese et al.*, 1994] as a primary timescale. We then correlated methane and $\delta^{18}O_{atm}$ variations in GISP2 with similar variations in Taylor Dome to place GISP2 and Taylor Dome on a common temporal framework. Doing so is complicated by the fact that gases trapped in polar ice are younger than the surrounding ice matrix, while the layer counting timescale provides ages for the ice matrix only. Below we describe the correlation procedure and the approach taken to account for this effect.

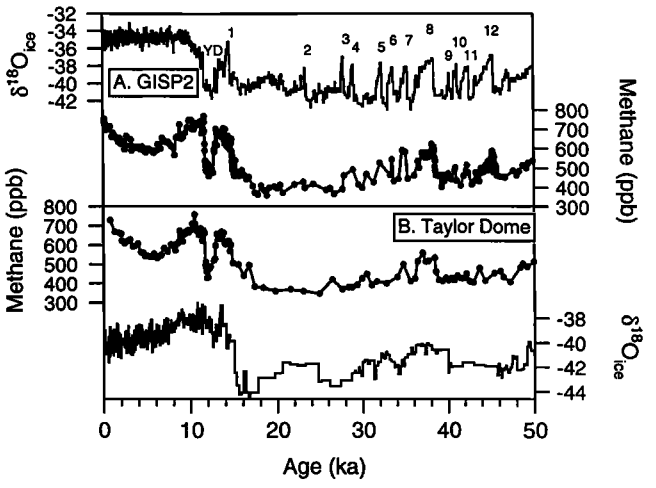

Figure 1. Methane and oxygen isotope records from (A) GISP2 and (B) Taylor Dome ice cores. Isotope data for GISP2 are 2 m averages from *Grootes et al.* [1993], and data for Taylor Dome are 0.5 m averages from *Steig et al.* [2000]. Numbered interstadials in the Greenland record are indicated in Figure 1. Timescales for GISP2 methane and isotope records are from *Brook et al.* [1996a]. Timescales for Taylor Dome methane and isotope records are described in the text.

3.2. GISP2 Gas Age Timescale and the Gas Age-Ice Age Difference

The depth at which air is trapped in polar ice (the close off depth) is a function of temperature and ice accumulation rate, and is typically 50-100 m below the ice surface. Above that depth, air is transported in the firn by convection and diffusion. Gases in polar ice are therefore younger than the surrounding ice. In Figure 1 we present methane results for GISP2 and Taylor Dome as a function of gas age. In this section and section 3.3 we explain how these timescales were derived.

For the GISP2 record we used the gas age timescale described by *Brook et al.* [1996a]. This timescale is based on the GISP2 layer counting timescale [*Meese et al.*, 1994], which provides ages for the ice matrix as a function of depth. GISP2 gas ages were calculated using the steady state *Herron and Langway* [1980] densification model [Brook et al., 1996a]. This model allows us to calculate the depth at which air bubbles were isolated from the atmosphere and the age of the air bubbles at that point, as a function of temperature and accumulation rate. This value is referred to as the gas age-ice age difference, or "Δ age." The gas age timescale is obtained by subtracting Δ age, which varies with time, from the ice age timescale. The GISP2 gas age scale used here agrees well (± 100 years) with a later GISP2 gas age timescale of *Schwander et al.* [1997], which incorporates gas age-ice age differences calculated from a dynamic densification model [*Barnola et al.*, 1991].

3.3. Correlation of Taylor Dome and GISP2 Timescales

For Taylor Dome we created a correlation gas age timescale by visually matching common inflection points in the GISP2 and Taylor Dome methane and $\delta^{18}O_{atm}$ time series, each corresponding to a time when methane or $\delta^{18}O_{atm}$ was changing rapidly, and interpolating between those points [*Sucher*, 1997; *Steig et al.*, 1998]. Because the atmosphere mixes in about a year, and the lifetimes of methane and oxygen in the atmosphere are longer, inflections in the methane or $\delta^{18}O_{atm}$ records should occur at essentially the same time in both polar regions. Using methane for correlation is complicated slightly by the existence of an interpolar methane gradient. We accounted for this complication by making the a priori assumption that the gradient was linearly proportional to the methane concentration over the time period of interest. We assumed that there was no gradient when methane concentrations were at their lowest levels and that the ratio of Greenland/Antarctic concentrations was 1.10 at the maximum concentration observed. The latter figure is based on earlier work [*Rasmussen and Khalil*, 1984] and the assumption of no gradient at times of low concentrations is equivalent to assuming no boreal methane sources at those times.

To correlate the records we created a gradient-adjusted Taylor Dome methane time series using these assumptions. The resulting control points are listed in Table 1. Below we calculate interpolar methane gradients with our data by averaging concentrations from both records over time periods during which methane levels were relatively stable. The assumption made above about the interpolar methane gradient does not influence

Table 1. Gas Age Control Points for the Taylor Dome Timescale for 50-0 ka: Correlation with GISP2 Atmospheric Methane and $\delta^{18}O_{atm}$ Records.

Depth, m	Age based on gas Correlation, ka bp	Correlated Variable
59.0	0.0	0-age depth in firn
285.5	5.9	methane
334.5	8.3	methane
339.0	8.8	methane
341.6	8.9	methane
356.2	10.9	$\delta^{18}O_{atm}$
358.3	11.3	methane
362.1	11.7	methane
370.2	12.4	$\delta^{18}O_{atm}$
370.6	12.8	methane
371.5	12.9	methane
377.5	14.9	methane
379.5	17.4	methane
384.2	26.3	$\delta^{18}O_{atm}$
398.0	34.2	methane
401.0	35.3	methane
404.0	36.3	methane
411.2	38.5	methane
461.7	56.7	$\delta^{18}O_{atm}$

Methane data from *Brook et al.* [1996a] and this work; $\delta^{18}O_{atm}$ from *Sucher* [1997].

those calculations because we correlate only at times of rapidly changing methane concentrations and do not calculate gradients for those times.

The uncertainty of the resulting Taylor Dome gas age timescale relative to the GISP2 gas age timescale is a function of the resolution of the records and varies with time. We estimate the uncertainty as one-half the sample resolution of the Taylor Dome record (which has lower sample resolution than GISP2); ± 100 years for 10-15 ka, ± 1000 years between 15 and 35 ka, and ± 500 years between 35 and 50 ka. Later than 8 ka we have very little age control in this timescale. Because accumulation rates probably varied between the control points and time periods between control points are large for some intervals, uncertainties at times between the match points are harder to quantify. At this level the accuracy of the correlation between Taylor Dome and GISP2 is not central to the interpretation of our results and is discussed further by *Steig et al.* [1998].

The ice age timescale for Taylor Dome (used to plot isotope records in Figures 1 and 3) is based on the gas age timescale described above. To determine ice ages we calculated Δ age using the *Herron and Langway* [1980] model, with temperatures inferred from the oxygen isotope record and accumulation rates inferred from measurements of ^{10}Be [*Steig*, 1996, *Steig et al.*, 1998]. We added Δ age to the gas ages to compute ice age as a function of depth. Uncertainties in the Taylor Dome ice age timescale are larger than those for the gas age timescale because they include uncertainty in Δ age due to imperfect knowledge of past firn conditions (i.e., temperature, accumulation rate, densification history). However, in this paper we consider only the gas records, for which these uncertainties are not critical. The interpretation of the timing of events in the Taylor Dome paleotemperature record and additional aspects of ice age timescales are discussed elsewhere [*Sucher*, 1997; *Steig et al.*, 1998, 2000].

4. Results and Discussion

4.1. Rapid Methane Variations During the Past 50,000 Years

4.1.1. Patterns of variation. In Figure 1 we present the GISP2 and Taylor Dome methane records for the past 50,000 years as well as isotopic records ($\delta^{18}O_{ice}$) from the GISP2 [*Grootes et al.*, 1993] and Taylor Dome [*Steig et al.*, 1998; 2000] ice cores. The general methane trends over this time period are known from previous work [*Chappellaz et al.*, 1990, 1993a, 1997; *Blunier et al.*, 1995; *Brook et al.*, 1996a]. Between 50 and 26 ka, several oscillations in methane concentration occurred synchronously or near-synchronously with $\delta^{18}O_{ice}$ variations observed in Greenland ice cores. Methane remained low (~400 ppb) between 26 and 17 ka, began rising slowly at 17 ka, rose rapidly at the beginning of the Bølling-Allerød period (starting at 14.8 ka), and remained at interglacial levels of 600-700 ppb for the next ~2000 years. The methane oscillation during the Younger Dryas [*Chappellaz et al.*, 1990] is also observed in both of our records, as is the prominent methane minimum during the mid-Holocene [*Blunier et al.*, 1995]. In general, where they overlap, our results agree well with those of *Chappellaz et al.* [1997], after correcting for a known interlaboratory offset of 2 % due to differences in standard gases [*Sowers et al.*, 1997].

4.1.2. Timing and rate of millennial-scale methane change. The Younger Dryas data (Figure 2) show that the rapid methane rise at the end of the Younger Dryas in the GISP2 record occurred within ± 100 years of the associated $\delta^{18}O_{ice}$ rise, but exact phasing can not be determined from these data because of uncertainties in gas age-ice age differences. Further work by *Severinghaus et al.* [1998] independently inferred the timing of the surface warming from anomalies in the $\delta^{15}N$ of N_2 in ice core air. These anomalies are caused by thermal isotopic fractionation in the firn due to the temperature gradient between the warm surface and the cooler close-off depth. *Severinghaus et al.* [1998] showed that the methane increase at the end of the Younger Dryas began 0-30 years after the temperature rise indicated by $\delta^{18}O_{ice}$.

We now also have high resolution methane data for the Bølling onset and the onsets of Interstadials 8 and 12 (Figure 2). In Figure 2 it appears that the start of the methane rise at the Bølling transition was coincident, within ~100-200 years, with the major shift in $\delta^{18}O_{ice}$ at 14.8 ka. The small apparent lead of methane relative to the major isotopic shift is ambiguous given uncertainty in the gas age-ice age difference and difficulty in identifying the start of the warming trend. New $\delta^{15}N$ results from the Bølling-Allerød transition indicate that the methane rise began ~20-30 years after the temperature rise [*Severinghaus and Brook*, 1999]. At the beginning of interstadial 8 methane apparently lead the change in $\delta^{18}O_{ice}$ by ~100 years (Figure 2), again within the uncertainty in the gas age-ice age difference. At the beginning of interstadial 12 the apparent lead of methane versus $\delta^{18}O_{ice}$ (~300 years) is larger than our estimate of Δage uncertainty. Clarification of the phasing of temperature and methane at these transitions awaits further measurements of $\delta^{15}N$ of N_2, which will provide precise information about their relative timing. Nonetheless, at all four transitions we studied in detail it appears that the rise in methane took place over one to three centuries, slower than associated changes in climate inferred from $\delta^{18}O_{ice}$ records and records of snow accumulation rate (R. Alley, personal communication, 1999). This result is discussed in section 4.1.3.

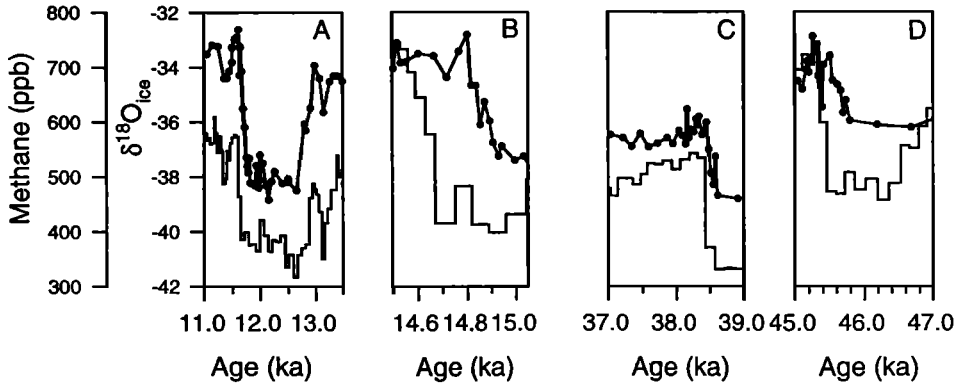

Figure 2. GISP2 methane and isotope data for (A) Younger Dryas, (B) Bølling transition, (C) Interstadial 8, and (D) interstadial 12. Methane data are plotted as filled circles; $\delta^{18}O_{ice}$ data are plotted as thin solid line. Apparent leads/lags between methane and the isotope records are within the uncertainty of the gas age timescale for GISP2, with the exception of Interstadial 12 (Figure 2d; see text).

4.1.3. Submillennial methane variations. Our results also indicate that between 20 and 10 ka, smaller scale methane variations occurred coincident with similar features in the ice core $\delta^{18}O_{ice}$ records (Figure 3). In the GISP2 $\delta^{18}O_{ice}$ record, three brief cold phases have been noted during this time period [Stuiver et al., 1995]. These have been correlated with the first phase of the Oldest Dryas, the Older Dryas, and the InterAllerød Cold Period (IACP) chronozones (Figure 3). In addition, there is a small negative $\delta^{18}O_{ice}$ oscillation at ~11.5 ka (Figure 3) in the preboreal period (Preboreal Oscillation or PBO) that has been noted

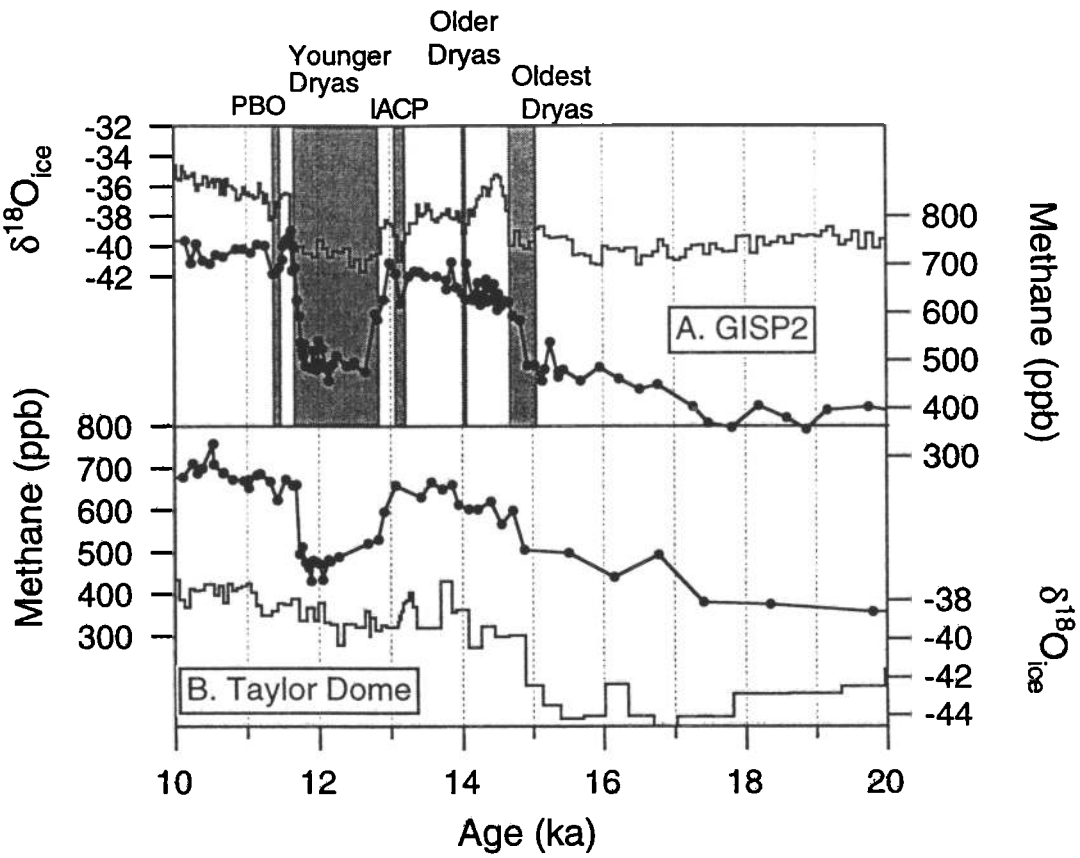

Figure 3. (A) GISP2 and (B) Taylor Dome methane and isotope records for the time period 20-10 kyr and correlation of cold substages in latest Quaternary with the GISP2 isotope record [*Stuiver et al.*, 1995]. The cool period in the early Preboreal (Preboreal Oscillation or PBO), which is associated with a small minimum in methane, was not discussed by Stuiver et al [1995] but is prominent in a number of paleoclimate records (see text). The fact that methane apparently increased before the $\delta^{18}O_{ice}$ temperature proxy is an artifact of uncertainty in the gas age-ice age difference (see text for further discussion)

in other high-latitude Northern Hemisphere paleoclimate records [e.g., *Lehman and Keigwin*, 1992). The GISP2 methane record contains small oscillations that appear to correspond with the Oldest Dryas, IACP, and the PBO (Figure 3). The Older Dryas, the smallest and shortest of these four events, is not clearly evident in the methane record. All of these features are relatively small, but similar minima that may correspond to the IACP and the PBO are possibly present in the Taylor Dome methane record (Figure 3). The coincidence of small minima in methane with these small isotopic temperature transients in GISP2 suggests that climate may have changed over broad geographic areas during these events, as during the larger interstadial events. *Hughen et al.* [1996] made a similar conclusion from analysis of varved sediments in the Cariaco Basin. They studied high resolution records of sediment reflectivity (grey scale) which reflect variations in the organic carbon content of sediments and the relative importance of dry, upwelling conditions and wet non-upwelling conditions in the trade wind belt north of Venezuela. These records are interpreted as proxies of tropical Atlantic trade wind strength and precipitation. Hughen et al. found oscillations in the gray scale record corresponding to the four events discussed above, suggesting that the tropical Atlantic experienced greater trade wind activity and lower precipitation during these brief cold events. Drier conditions in the tropics would likely result in lower methane emissions from tropical wetlands.

4.2. Rate and Magnitude of Methane Change During Rapid Climate Transitions

Methane variations observed in ice cores on all timescales (with the exception of the recent industrial period) have a maximum range of ~400 ppb and have primarily been viewed as tracers of temperature and precipitation in wetland regions [*Chappellaz et al.*, 1990, 1993a; *Brook et al.*, 1996a). Alternative views suggest that rapid, and large, atmospheric methane variations may have been caused by catastrophic release of methane from methane hydrates in marine sediments and that these large emissions might have forced or amplified rapid climate change [*Nisbet*, 1992, *Kennett et al.*, 1996; *Thorpe et al.*, 1996]. Such events could have been rapid enough that they have not been observed at the resolution of previous ice core methane records [*Thorpe et al.*, 1996]. In this section and section 4.3 we use our results to examine these ideas.

The four transitions we examined in detail have similar characteristics (Figure 2). Concentrations rose rapidly from "stadial" levels of 450-500 ppb to "interstadial" levels of 600-770 ppb (Figures 1 and 2). The transitions were generally smooth, but some one-point reversals are evident during the Younger Dryas and interstadial 8. Once interstadial conditions were reached, methane concentrations stayed high for roughly the duration of the warming event (with the exception of interstadial 12) (Figures 1 and 2). However, we note that methane and isotopic temperature do not track each other perfectly. During the Bølling-Allerød period, for example, temperatures inferred from $\delta^{18}O_{ice}$ fell gradually over the time period from 14.5 to 13.0 ka, while methane concentrations rose gradually. We also note that during interstadial 12, approximately 300 years after the beginning of the methane rise (Figure 2), there is a negative oscillation in methane that lasted for ~ 200 years. This feature does not seem to correspond to any significant event in the GISP2 $\delta^{18}O_{ice}$ record (Figure 2), which has a resolution of ~ 80-100 years. Additional $\delta^{18}O_{ice}$ data increase the resolution to ~ 40-50 years over this interval, but do not reveal a similar oscillation [M. Stuiver, personal communication, 1998]. However, a similar oscillation is found in an alkenone-based sea surface temperature proxy from a high resolution marine sediment record at the Bermuda Rise [*Sachs and Lehman*, 1999], suggesting that this methane oscillation may be the result of a real climate event.

It is important to consider the extent to which these data represent the true atmospheric history during these short-term events. Two processes affect the relationship between the true atmospheric methane history and the ice core methane record. First, gases mix by diffusion in the firn layer. This process smoothes the atmospheric history and has been modeled by *Schwander et al.* [1993; 1997], *Battle et al.* [1996], and *Trudinger et al.* [1997]. The age distribution of gas molecules at the depth of gas trapping can be calculated with appropriate diffusion models. The width of the age distribution depends on temperature, accumulation rate, and meteorological conditions that control the thickness of a convective zone in the upper several meters of the firn [*Schwander et al.*, 1997]. Under modern conditions at GISP2, the width of the age distribution at half-height is ~ 10 years [*Schwander et al.*, 1997].

Second, the bubble close-off process that occurs when firn transforms to ice is not instantaneous but happens over a finite depth interval, potentially introducing additional smoothing of the gas record. A number of studies indicate that gas mobility near the firn-ice transition is low owing to early close off of wintertime layers [*Etheridge et al.*, 1992; *Martinerie et al.*, 1992; *Schwander et al.*, 1993; *Battle et al.*, 1996]. As a result, this second process is not expected to add additional smoothing to the methane record at the GISP2 site [*Schwander et al.*, 1993; 1997].

We calculated the smoothing effect of firn diffusion using a numerical diffusion model [*Severinghaus et al.*, 1998] that calculates the concentration or isotopic composition of a gas species at the depth of bubble close off. The model is time dependent and includes the effects of concentration diffusion, gravitational settling, and thermal diffusion. Gas diffusivities were based on a density-depth relationship and empirical density-diffusivity relation derived from CO_2 measurements in South Pole firn air [*Battle et al.*, 1996]. Methane diffusivity was assumed to be 1.35 times the CO_2 diffusivity [*Schwander et al.*, 1993]. We predicted the age distribution of air trapped during the large climate shift at the end of the Younger Dryas (Figure 4) by forcing the model with a delta function and examining the resulting time series of concentrations at the lock-in zone. Temperature and accumulation rate boundary conditions were based on Younger Dryas conditions as described by *Severinghaus et al.* [1998]. The predicted age distribution at the base of the firn has a width at half-height of ~ 20 years (Figure 4). This value is a conservative maximum because the model contained no near-surface convective zone; convection would reduce the width of the age distribution.

In the GISP2 record, methane concentrations rose at the end of the Younger Dryas, the start of the Bølling period, and at the onsets of interstadials 8 and 12, over time periods of 100-300 years (Figures 2 and 3). In contrast, the associated temperature shifts inferred from the $\delta^{18}O_{ice}$ ice record (Figure 2), are several decades long at most, and records of snow accumulation rate at the GISP2 site also suggest extremely rapid changes in climate for many of these transitions [*Alley et al.*, 1993; R. Alley,

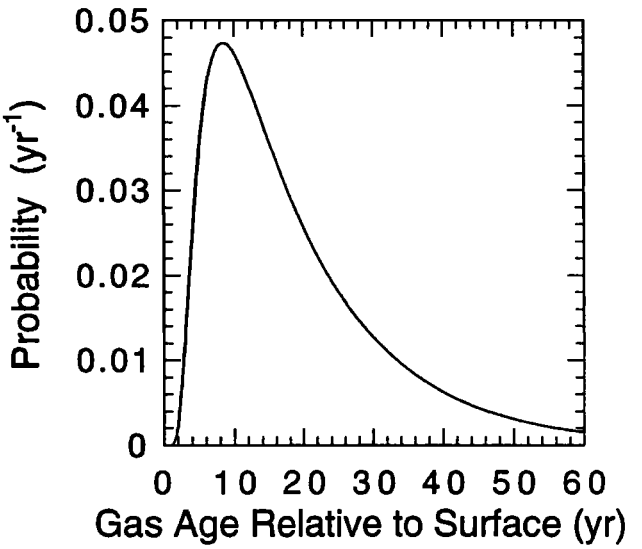

Figure 4. Modeled age distribution of air trapped at the base of the firn at the GISP2 site under Younger Dryas conditions. Age distribution was calculated with a firn diffusion model that is described in the text.

personal communication, 1999]. The data for all four transitions show that the time for methane to rise from stadial to interstadial values is longer than the width of the age distribution (~20 years). Therefore the ice core concentration histories presented here are true representations of atmospheric history, with the exception that changes occurring over one to two decades or less are smoothed (Figure 5). This conclusion is verified by the fact that faster, decadal variations of $\delta^{15}N$ of N_2 in trapped air in GISP2 are preserved in ice of similar age [*Severinghaus et al.*, 1998; *Severinghaus and Brook*, 1999].

4.3. Origin of Rapid Changes in Methane?

4.3.1. Emission from terrestrial ecosystems. One explanation for the longer timescale for rising methane levels may be that changes in the temperature and hydrologic cycle in tropical or temperate regions occurred on a slower timescale than rapid temperature shifts recorded in high-latitude ice cores. However, some tropical records suggest equally rapid climate shifts at this time. For example, in their study of the Carioco Basin climate record (discussed in section 4.1.3), *Hughen et al.* [1996] concluded that the event correlative to the Younger Dryas termination occurred in less than a decade. A second possible explanation for the slower methane response is that the century timescale for the methane rise is related to ecological changes forced by climate change. Changes in methane emissions from wetlands during these climate transitions may have involved changes in primary productivity, species composition, and other ecosystem dynamics that influence methanogenesis. The slower timescale for methane increases may represent a lag in the response of these processes to climate change [e.g., *Prentice*, 1986; *Webb*, 1986; *Campbell and McAndrews*, 1993]. This hypothesis is supported by terrestrial evidence that indicates rapid, large changes in vegetation patterns occurred in a variety of regions, including the tropics, on centennial timescales at the Younger Dryas, Bølling, and other interstadial transitions [*Lowe et al.*, 1994; *Allen et al.*, 1999]. The lag in methane response may also reflect changes in the hydrologic balance in wetland regions at the beginning of interstadial events. If climate shifted to wetter conditions at the beginning of interstadial events, several decades might have elapsed before rising water tables could saturate surface or near-surface soils and promote anaerobic conditions.

4.3.2. Methane hydrates. We suspect that massive destabilization of methane hydrates in marine sediments or permafrost would likely lead to more rapid and larger changes in the methane concentration than we observe in our records. For example, *Thorpe et al.* [1996], in a comprehensive treatment of this problem, modeled a 4000 Tg (4000 Tg is roughly 20 times the pre-industrial methane budget) burst of methane in the high-latitude Northern Hemisphere with a 2-D atmospheric circulation and chemistry model. They showed that such an instantaneous release would cause a rapid rise in methane concentration reaching maximum levels within a few years. In their model this event produced atmospheric methane concentrations in excess of 2000 ppb in the Northern Hemisphere and locally in excess of 25,000 ppb immediately after the event. Although such high concentrations are not observed in any existing ice core methane records, brief periods of elevated methane concentration might not have been recorded in previous records given their limited resolution (> 100 years) [*Thorpe et al.*, 1996].

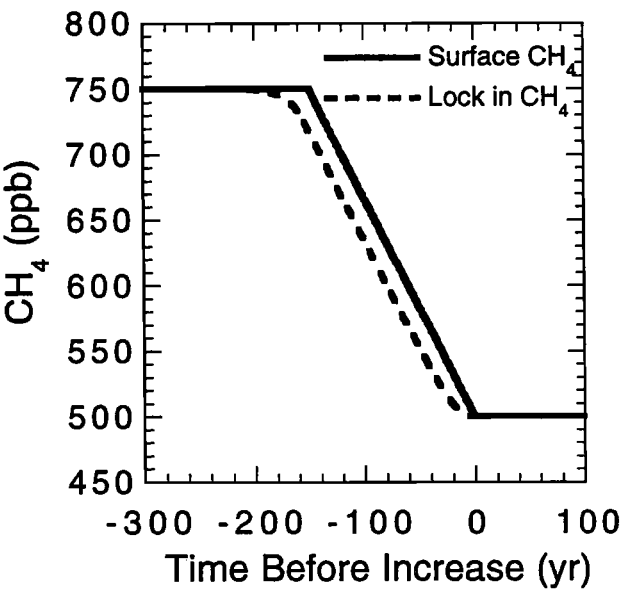

Figure 5. Illustration of the effect of mixing in the firn on ice core methane record using the firn diffusion model of *Severinghaus et al.* [1998] for conditions at the end of the Younger Dryas. "Surface" indicates the hypothetical atmospheric methane history; "lock in" indicates the methane history recorded by the ice core. Smoothing of the ice core methane record by diffusion does not significantly influence the ice core recording of the magnitude or apparent speed of transitions in atmospheric methane concentration that take more than ~ 100 years. Therefore apparent uniform transitions of this length or longer represent the true rate of change of atmospheric methane at the surface of the ice core location. The offset between the hypothesized atmospheric history and that recorded by the ice core record is ~10-20 years and represents the time necessary for an atmospheric signal to diffuse to the base of the firn.

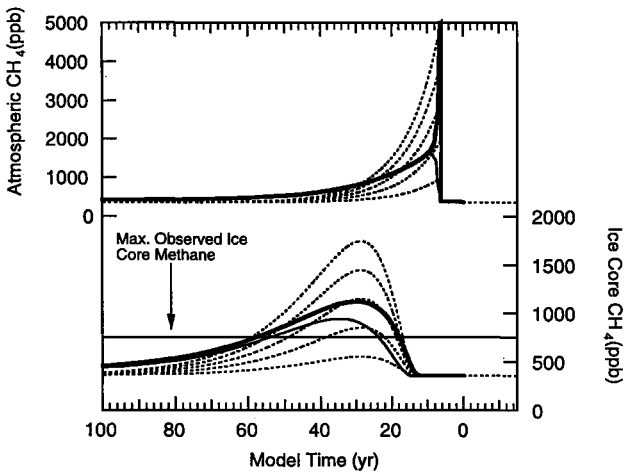

Figure 6. Model simulations of instantaneous release of methane from clathrates to the atmosphere and the ice core response to those events. The ice core response was calculated by convolving the age distribution shown on Figure 4 with the hypothetical atmospheric histories. Thin dashed lines are step functions in the atmospheric methane concentration, from 350 ppb to 1000, 2000, 3000, 4000, and 5000 ppb, from top to bottom, respectively, assuming no change in atmospheric methane lifetime (10 years) and simple exponential decay of initial concentration. Heavy solid line shows results from the *Thorpe et al.* [1996] model of a clathrate release event at 66°N in the Northern Hemisphere, thin solid line represents the response of the high latitude Southern Hemisphere (e.g., the latitude of Taylor Dome) to that event [*Thorpe et al.*, 1996].

In Figure 6 we plot hypothetical ice core concentration histories arising from instantaneous releases of methane to the atmosphere. To calculate these we smoothed hypothetical atmospheric histories by convolution with the predicted age distribution shown in Figure 4. This age distribution was calculated for conditions at the end of the Younger Dryas period and should approximate the age distribution at other transitions. We first plot five simple concentration histories based on instantaneous increases of methane levels to values of 1000-5000 ppb, and subsequent decrease in concentration using the current atmospheric lifetime of 10 years. In reality, the lifetime would probably increase with the emission of this much methane, owing to a corresponding decrease in atmospheric OH, the principle methane sink. Using the modern lifetime in our sensitivity calculations decreases the length of time that concentrations remain high, providing a conservative comparison with our data. This simple analysis (Figure 6) shows that the high-resolution ice core record is inconsistent with the large and rapid change in atmospheric methane concentrations that an instantaneous release would produce. Smoothing in the firn gives an instantaneous event an apparent duration of ~ 20 years, while the data show that methane concentrations rose over time periods of 100-300 years at the four transitions we examined in detail.

In Figure 6 we also plot the model atmospheric history for the 4000 Tg release at high northern latitudes (66°N) from *Thorpe et al.*, [1996], and our predicted ice core response. Examination of these results leads to a similar conclusion. The GISP2 methane record is not consistent, in magnitude or in speed, with an instantaneous release of large quantities of methane to the high-latitude Northern Hemisphere at the initiation of interstadial events. However, clathrate bound methane might be released from other locations [*Thorpe et al.*, 1996; *Kennet et al.*, 1996]. While our results appear to rule out significant clathrate release in the Northern Hemisphere, a similar event in the Southern Hemisphere might not produce as dramatic a concentration history at the GISP2 site due to atmospheric mixing (Figure 6) [*Thorpe et al.*, 1996]. The Taylor Dome methane results have a lower resolution than the GISP2 data and cannot be used to entirely rule out a Southern Hemisphere or perhaps mid-latitude clathrate release. To address this issue we employ Thorpe et al.'s predicted Southern Hemisphere atmospheric response to their clathrate release in the Northern Hemisphere (Figure 6) as a crude analog for the response of the high-latitude Northern Hemisphere to a clathrate release at high southern latitudes. For simplicity we assume that atmospheric mixing and chemical processes are latitudinally symmetrical. The ice core response to such an event would be an apparent rise in methane of ~ 15 year duration (Figure 6), again, much faster than observed in our data.

As discussed by *Chappellaz et al.* [1997], we cannot exclude a slower and smaller release of clathrate methane as the source for the atmospheric methane concentration changes we observe. However, we can rule out rapid, large changes in methane concentrations that would provide significant radiative climate forcing for the rapid changes in temperature observed at the beginning of interstadial events. Our data suggest that the changes in methane concentration in the ice core record (e.g., shifts from 350-400 ppb to 600-700 ppb) closely represent the true atmospheric history. These changes are generally believed to be too small to contribute significantly to the several degrees of warming that occurred at the beginning of interstadial events and the end of the Younger Dryas [*Raynaud et al.*, 1988; *Chappellaz et al.*, 1993a].

Finally, our results show that high methane concentrations were maintained throughout the Preboreal, Bølling-Allerød, and interstadial 8 periods. In these three cases, century-long rises in methane concentration were followed by periods of elevated concentrations that lasted 1000 years or longer, roughly the same length of time as the warming event (Figure 2). Interstadial 12 is an exception, as it consists of the previously discussed brief decrease in concentration after the initial warming, a subsequent return to high concentrations, then a gradual decline. High-resolution data for ~500 years after all of these warmings (Figure 2) show that methane concentrations for the most part remained within an envelope of ~ 50 ppb during these events (again with the exception of interstadial 12), with temporal resolution as short as 20 years for the Younger Dryas termination and the beginning of the Bølling-Allerød. We find no evidence of periodic, large injections of methane from clathrate destabilization during these time periods.

4.4. Interpolar Gradient

The majority of modern natural methane emissions originate in two major latitude bands; a high-latitude region between 50°-70°N (primarily emissions from boreal wetlands) and a low latitude region in the tropics of both hemispheres (primarily emissions from tropical wetlands) [*Fung et al.*, 1991; *Hein et al.*, 1997]. In the pre-industrial atmosphere (250-400 years ago) the methane concentration in the high-latitude Northern Hemisphere was 8-10% higher than in the high-latitude Southern Hemisphere

[*Rassmussen and Khalil*, 1984; *Nakazawa et al.*, 1993]. This latitudinal dependence of the concentration reflects a dominance of Northern Hemisphere sources in the preindustrial Holocene and the fact that the atmospheric lifetime of methane (~10 years) [Prinn et al., 1995] is of the same order as the mixing time between hemispheres (~1 year). The concentration difference between the northern and southern high latitude regions can be reconstructed for past times from ice cores [*Rasmussen and Khalil*, 1984; *Brook et al.*, 1996b; *Chappellaz et al.*, 1997] and has been called the interpolar gradient (IPG). The IPG has been defined in a variety of different ways [*Rasmussen and Khalil*, 1984; *Nakazawa et al.*, 1993; *Chappellaz*, 1997]. Here we define it as

$$IPG=(C_N/C_S-1) \quad (1)$$

where C_N is the atmospheric concentration in Greenland and C_S is the concentration in Antarctica. Positive values indicate higher concentrations in the Northern Hemisphere, negative values indicate higher concentrations in the Southern Hemisphere.

Figure 7 shows the methane records for the last 40 ka from Taylor Dome and GISP2. To calculate the IPG for past times we determined average concentrations at the Greenland and Antarctic core sites during time periods when methane concentrations were relatively stable [*Chappellaz et al.*, 1997]. Doing so avoids problems with inaccuracies in chronology which would affect IPG most significantly during times of rapidly changing concentrations. Time-weighted mean concentrations were calculated for these time periods following *Chappellaz et al.* [1997], and the IPG was calculated from the appropriate pair of means (equation 1). The time periods examined, mean concentrations, and IPGs are listed in Table 2. For the 5-7 ka period during the mid-Holocene, the Taylor Dome timescale is not defined precisely. Therefore rather than using a time-weighted mean we chose a single value from both cores, the minimum concentration measured for that period.

The IPGs are plotted in Figure 7. Also shown are IPGs from the GRIP (Greenland), Byrd (Antarctica), and D47 (Antarctica) ice core records, recalculated from the data of *Chappellaz et al.* [1997]. Their results cover the later part of the Holocene and overlap our estimates for the mid-Holocene and Preboreal. Our results for the Preboreal period are in good agreement with those of *Chappellaz et al.* [1997]. Our value for the mid-Holocene is very close to that determined by Chappellaz et al. for the time period 2.5-5 ka but is higher than that for the preceding period.

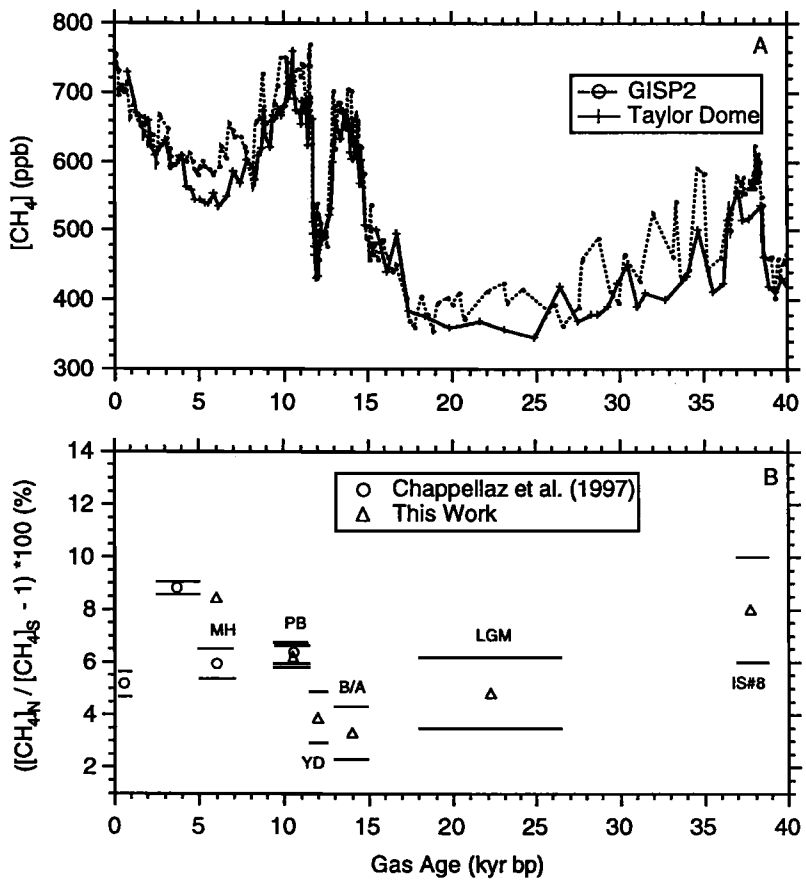

Figure 7. (A) Methane records for the GISP2 and Taylor Dome cores over the last 40 ka. (B) Mean interpolar gradients (IPG) for selected time periods based on the GISP2 and Taylor Dome data and also reproduced from *Chappellaz et al.* [1997]. We define IPG as $[C_N/C_S]$-1, where C_N is the Northern Hemisphere (Greenland) methane concentration and C_S is the Southern Hemisphere (Antarctic) methane concentration. The length of the horizontal bars illustrates the time period over which the mean value is calculated, and the vertical range represents the 2σ uncertainty in the mean. See text for details.

Table 2. Weighted Mean Methane Concentrations for Interpolar Gradient Calculation.

	Time Interval ka bp	Greenland	Antarctica	IPG, %
Mid-Holocene*	5-7	579±12	534±11	8.4±0.5
Number of depths		1	1	
Preboreal	9.5-11.5	720±4	678±4	6.2±0.4
Number of depths		32	23	
Younger-Dryas	11.5-12.5	495±5	476±6	3.9±1.0
Number of depths		19	12	
Bølling-Allerød	13.5-14.8	646±6	625±9	3.2±1.0
Number of depths		41	12	
Last Glacial Max	18-26	395±5	377±7	4.8±1.4
Number of depths		15	11	
Interstadial 8	37-39	576±5	533±10	8.0±2.0
Number of depths		22	4	

The error for the methane concentration is 1 weighted standard deviation of the mean as defined by *Chappellaz et al.* [1997]. The error for the IPG is the 95% confidence interval.
*These values are not time-weighted means but are the minimum values for this period. Uncertainty based on 2% error (general agreement between replicate ice samples) for each measurement.

Comparison here is difficult due to dating uncertainties for Taylor Dome. The results show that the IPG was generally lower during the Last Glacial Maximum (LGM), Bølling-Allerød, and Younger Dryas, suggesting a dominance of tropical sources. The IPG increased at the beginning of the Preboreal period (Figure 7), suggesting that northern sources became more significant immediately after the end of the Younger Dryas. The value for interstadial 8 (8 ± 2%) is similar to that during the mid-Holocene, suggesting substantial Northern Hemisphere sources during this event, which occurred during the middle portion of the Marine Isotope Stage 3 (Table 3). This result is preliminary owing to the limited data from the Taylor Dome core. Variations in the IPG during the Holocene are discussed in detail by *Chappellaz et al.* [1997].

4.5. Implications of IPG for Methane Source Distribution

The IPG is controlled by the latitudinal distribution of methane sources, the latitudinal distribution of methane sinks, and the mixing rates within and between hemispheres. If the sink distribution and mixing rate are assumed to remain constant over time (or if their temporal variations are known), a box model may be used to estimate changes in the source distribution [*Khalil and Rassmussen*, 1983; *Rassmussen and Khalil*, 1984; *Chappellaz et al.*, 1997]. The model divides the troposphere into three boxes, the North (N; 30°-90°N), the Tropics (T; 30°S-30°N), and the South (S; 30°-90°S). Boxes N and S represent 25% each of the total tropospheric volume, and box T represents 50% of the volume of the troposphere. The mass balance is described by

$$\mathbf{dC/dt=F-\Omega C} \tag{2}$$

where **C** (Tg box^{-1}) is a vector representing the atmospheric methane concentration in each box and **F** (Tg yr^{-1}) is a vector representing the methane source in each box. The sink (primarily oxidation by OH in the troposphere) is represented by **ΩC** where

$$\Omega(yr^{-1}) = \begin{bmatrix} \lambda_N + n_N & -n_N/2 & 0 \\ -n_N & \lambda_T + (n_N + n_S)/2 & -n_S \\ 0 & -n_S/2 & \lambda_S + n_S \end{bmatrix} \tag{3}$$

Table 3. Methane Emissions Calculated From Three Box Model Using Taylor Dome and GISP2 Measurements (Table 2)

Period	Time Interval, ka bp	Methane Emissions (Tg/yr)* North	Tropics	South+	Total
Mid-Holocene	5-7	65±14	79±23	15	159
Preboreal	9.5-11.5	64±5	123±8	15	202
Younger-Dryas	11.5-12.5	39±6	86±11	15	141
Bølling-Allerrød	13.5-14.8	43±7	127±15	15	185
Last Glacial Max	18-26	34±6	65±9	12	111
Interstadial 8	37-39	63±7	80±11	15	158

*The error for the source estimate is the 95% confidence interval based on propagating errors from Table 2.
+Southern source is fixed (see text).

The coefficient for removal, λ (yr^{-1}), is defined as $1/t$ where t is the methane lifetime (year). The transport coefficient, n (yr^{-1}), is defined as $1/\tau$, where τ is the transport time between boxes. Assuming steady state, and with knowledge of t, τ, C, and the volumes of the boxes, the latitudinal source distribution can be calculated from (1). We used values for these parameters from *Chappellaz et al.* [1997] to make our results comparable with their calculations for later time periods. (The values are 9 months for τ_N and τ_S, and 15.6, 6.8, and 22.4 years for t_N, t_T and t_S, respectively).

The methane concentration in box S is considered homogeneous and is therefore well represented by measurements in the Antarctic core. Box N is not well mixed in the modern atmosphere. For example, in the compilation of *Fung et al.* [1991], the methane concentration increases linearly by ~ 60 ppb between 30°N and 90° N. The gradient within box N is at least partly a result of anthropogenic methane sources in the Northern Hemisphere, and must have been lower in the past. Following *Chappellaz et al.* [1997] we assume that the difference between the concentration at 70°N and the box N average is 7% of the total interhemispheric difference. Therefore, to calculate average concentrations for box N from Greenland concentration data, we decrease the Greenland concentration by 7% of the GISP2-Taylor Dome difference. In reality, the 7% value may have changed with time, but we are currently unable to constrain this effect accurately, and the correction is small in any case. The concentration for box T is not known but is determined in the model by fixing the southern source at 15 Tg yr^{-1} (12 Tg yr^{-1} for the LGM) [*Chappellaz et al.*, 1997]. These values may be slightly too high. *Fung et al.* [1991] indicate that natural sources in this latitude band today sum to ~ 11 Tg/yr, and *Hein et al.* [1997] derive a value of ~13 Tg yr^{-1}. However, such source estimates are difficult to construct and may have been higher prior to the industrial revolution. As long as this value is held constant, relative differences in source distribution are not significantly affected, but a real change in the southern source (for example between the Younger Dryas and Preboreal periods) would not be represented in our calculations. For example, considering the Younger Dryas-Preboreal transition, using a value of 10 Tg yr^{-1} rather than 15 Tg yr^{-1} for the target southern source changes the northern source by -5 Tg yr^{-1} and the tropical source by +10 Tg yr^{-1}. These changes are small relative to the magnitude of current uncertainties (Table 3).

As we have no direct constraints for a number of the parameters used in these calculations (e.g., transport time, lifetimes, and tropical concentration), the model results can only be used for a first-order interpretation of changes in the IPG. We use this model with the GISP2 and Taylor Dome methane data to estimate methane emissions for boxes N and T in the mid-Holocene, the Preboreal period, the Younger Dryas, the Bølling-Allerød, the LGM, and for a preliminary estimate for interstadial 8 (Table 3). For the Preboreal period our source estimates overlap with those of *Chappellaz et al.* [1997] (Figure 7) and are not statistically different (at 95% confidence using Students t test) from theirs. Our results for the mid-Holocene differ from those of Chappellaz et al. from adjacent time periods but are within the range established by their data. However, as mentioned above, the chronology of the Taylor Dome core is not adequately established in this time period.

The geographic distribution of methane emissions during the period we designated as LGM was similar to that during the Bølling-Allerød period, despite the ~ 200 ppb difference in concentration (Figure 7, Table 3). This suggests a doubling (roughly) of tropical source strength (Table 3), with little change in boreal source strength. Examination of the data in Figure 7, however, suggests that during the 2 ka period immediately prior to the Bølling increase, the interpolar gradient may have been reversed (e.g., Southern Hemisphere concentration higher). Although our data are insufficient for a precise gradient calculation for this time period, recent work by Dallenbach et al. [2000] confirms this suggestion and indicates that tropical sources increased by ~ 40 Tg yr^{-1} at the Bølling transition and boreal sources increased by ~ 30 Tg syr^{-1}. The total methane source immediately after the Bølling transition was ~ 175-185 Tg yr^{-1} by their calculations, similar to our value of 185 Tg yr^{-1}.

A global decrease in methane source strength occurred during the Younger Dryas, followed by an increase in Northern Hemisphere and tropical source strength at the beginning of the Preboreal period (Figure 7). The large difference in the IPG between the Bølling-Allerød and Preboreal periods is the most robust of our results, owing to the large number of data points in both periods. It requires that tropical methane sources were similar in magnitude (Table 3) but that boreal sources were about 50% higher during the Preboreal period. The results further suggest that expansion of Northern Hemisphere sources occurred at the very beginning of the Preboreal period (Figure 7). At the start of the Preboreal period substantial portions of eastern Canada and Fennoscandia remained ice covered [*Peltier et al.*, 1994]. Nonetheless, methane emissions from Northern Hemisphere sources must have expanded rapidly at the end of the Younger Dryas, perhaps due to formation of productive wetlands from high-latitude regions which were already ice free. The new methane source areas may have been in regions of Siberia that remained ice free during the glaciation or other areas that deglaciated early. The methane results imply that these regions experienced warm and wet conditions at this time, consistent with other evidence [e.g., *Ritchie et al.*, 1983; *Crowley*, 1991]. In summary, regardless of the specific location of these northern sources, the interpolar gradient data (Figure 7; Tables 2 and 3) suggest that tropical sources were a significant, though variable, component of the methane budget at all time periods over the past 50 ka.

The simple model used here does not account for possible changes in atmospheric mixing or chemical removal of methane from the atmosphere, both of which may have changed over the past 50 ka. For example, the methane lifetime during the preindustrial period, and particularly the glacial period, is not well constrained and may have been shorter than assumed in the model [*Thompson*, 1992]. Also, numerous studies have suggested that wind speeds were higher in glacial times, possibly resulting in greater interhemispheric mixing. We briefly explore the sensitivity of the model to these changes (Figure 8). For a given interpolar gradient, invoking faster atmospheric mixing (shorter transport time) increases the calculated northern source and decreases the calculated tropical source (Figure 8). Decreasing methane lifetime increases inferred source strength in northern or tropical boxes (Figure 8), although the effect is larger in the tropics due to the shorter lifetime. Considering the transition from the Younger Dryas to the Preboreal period, for example, a decrease in atmospheric mixing that was unaccounted for in the model would result in an overestimate of changes in northern source strength and an underestimate of changes in

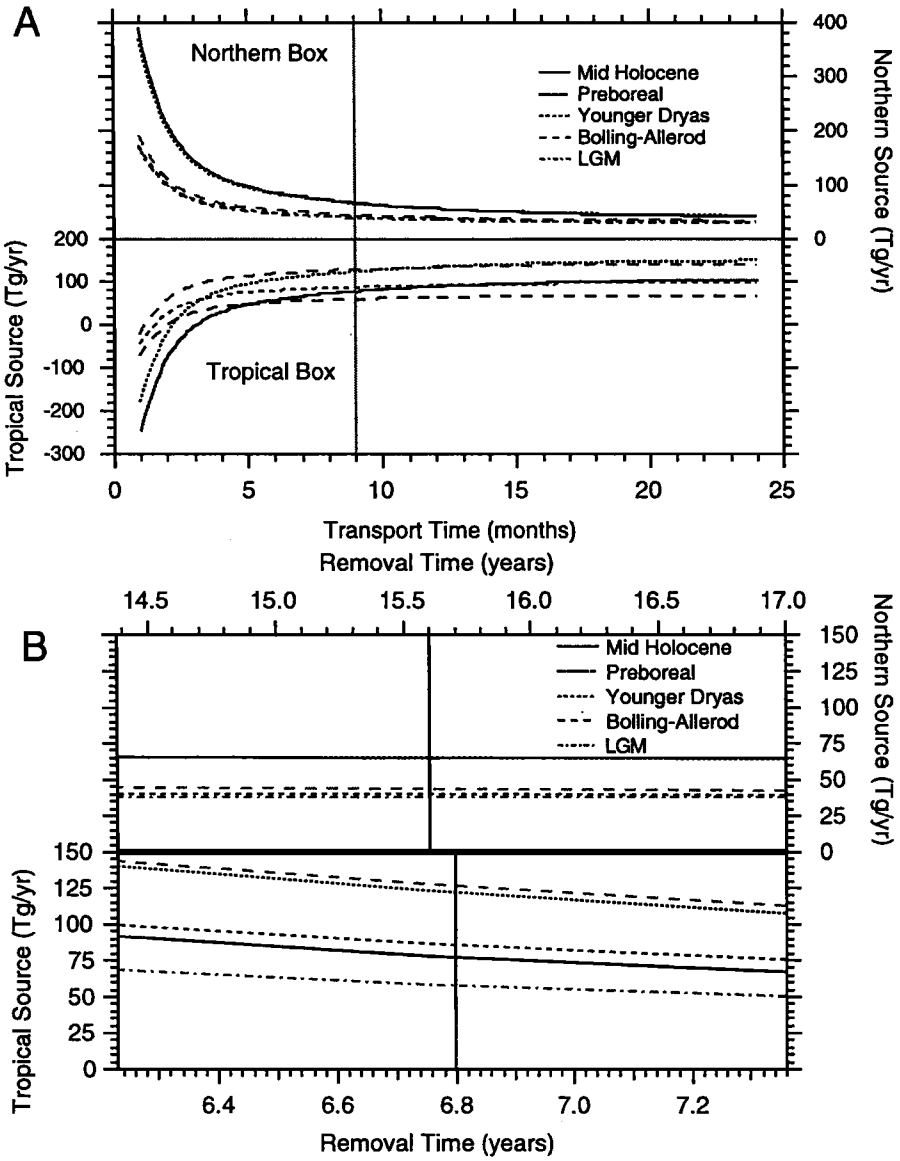

Figure 8. Dependence of model derived source strength in northern and tropical boxes on (A) transport time between boxes and (B) methane removal time. Model calculations used to produce these curves held methane emissions in the southern box at 15 Tg yr^{-1} (12 Tg yr^{-1} for LGM, see text). Vertical lines indicate the values of these parameters used in the three-box model.

tropical source strength. An increase in removal time for the same transition would result in an overestimate of changes in source strength in both boxes, but the effect is more significant in the tropics. How either variable changed in the past is not well known, but within a reasonably large range of mixing times and removal times the first-order results of our study are not grossly affected (Figure 8).

5. Conclusions

Models constrained by ice core methane measurements in both hemispheres for the time period 5-40 ka support the suggestion that changes in both tropical and boreal sources are required to explain observed rapid changes in methane concentration. Changes in only Northern Hemisphere sources would result in higher IPG values than observed. Our results and recent related work [Severinghaus et al., 1998; Severinghaus and Brook, 1999], also indicate that at least some of the increases in methane concentration occurred nearly synchronously with the onset of rapid warming events in the GISP2 stable isotope record. The magnitude and rate of change of methane concentrations appear to be inconsistent with a release of large quantities of methane from clathrates.

Acknowledgments. We thank Melissa Swanson and Joe Orchardo for laboratory assistance, Todd Sowers, Jerome Chappellaz, and Thomas Blunier for sharing methane data and Richard Thorpe for sharing atmospheric modeling results. Comments of two anonymous reviewers helped clarify many of our arguments. This work was supported by NOAA Climate and Global Change Postdoctoral Fellowships to Ed Brook, Susan Harder, and Jeff Severinghaus, and grants from the National Science Foundation including OPP-9714687 and OPP-972591.

References

Allen, J.R.M., et al., Rapid environmental changes in southern Europe during the last glacial period, *Nature, 400*, 740-743, 1999.

Alley, R., et al., Abrupt increase in Greenland snow accumulation at the end of the Younger Dryas event, *Nature, 362*, 527-529, 1993.

Barnola, J.M., P. Pimienta, D. Raynaud, and Y.S. Korotkevich, CO_2-climate relationship as deduced from the Vostok ice core: A re-examination based on new measurements and on a re-evaluation of the air dating, *Tellus, Ser. B, 43B*, 83-90, 1991.

Bender, M., T. Sowers, M.L. Dickson, J. Orchardo, P. Grootes, P. Mayewski and D. Meese, Climate connections between Greenland and Antarctica during the last 100,000 years, *Nature, 372*, 663-666, 1994.

Blunier, T., J.A. Chappellaz, J. Schwander, J.M. Barnola, T. Desperts, B. Stauffer, and D. Raynaud, Atmospheric methane record from a Greenland ice core over the last 1,000 years, *Geophys. Res. Lett., 20*, 2219-2222, 1993.

Blunier, T., J. Chappellaz, J. Schwander, B. Stauffer, and D. Raynaud, Variations in atmospheric methane concentration during the Holocene epoch, *Nature, 374*, 46-49, 1995.

Broecker, W. S., D. Peteet, I. Hajdas, J. Lin, and E. Clark, Antiphasing between rainfall in Africa's rift valley and North America's Great Basin, *Quat. Res., 50*, 12-20, 1998.

Brook, E., T. Sowers, and J. Orchardo, Rapid variations in atmospheric methane concentration during the past 110,000 years, *Science, 273*, 1087-1091, 1996a.

Brook, E.J., J.P. Severinghaus, M. Swanson, and P. Grootes, Late glacial methane variations in Greenland and Antarctic ice cores, *EOS, Trans. AGU, 77(17)*, Spring Meeting Supplement, S156, 1996b.

Brook, E.J., J. Severinghaus, S. Harder, and M. Bender, Atmospheric methane and millennial-scale climate change, in *Mechanisms of Global Climate Change at Millennial Timescales, Geophys. Monogr. Ser.*, vol. 112, edited by P. U. Clark, R. S. Webb, and L. Keigwin, pp. 165-176, AGU, Washington D.C., 1999.

Bubier, J., and T.R. Moore, An ecological perspective on methane emissions from northern wetlands, *Trends Ecol. and Evol., 9*, 460-465, 1994.

Campbell, I.D., and J.H. McAndrews, Forest disequilibrium caused by rapid Little Ice Age cooling, *Nature, 366*, 336-338, 1993.

Chappellaz, J., J.M. Barnola, D. Raynaud, Y.S. Korotkevich, and C. Lorius, Atmospheric methane record over the last climatic cycle revealed by the Vostok ice core, *Nature, 345*, 127-131, 1990.

Chappellaz, J., T. Blunier, D. Raynaud, J.M. Barnola, J. Schwander, and B. Stauffer, Synchronous changes in atmospheric methane and Greenland climate between 40 and 8 kyr BP, *Nature, 366*, 443-445, 1993a.

Chappellaz, J.A., I.Y. Fung and A.M. Thompson, The atmospheric methane increase since the last glacial maximum, 1, Source estimates, *Tellus, Ser. B, 45B*, 228-241, 1993b.

Chappellaz, J., T. Blunier, S. Kints, B. Stauffer, and D. Raynaud, Variations of the Greenland/Antarctic concentration difference in atmospheric methane during the last 11,000 years, *J. Geophys. Res., 102*, 15,987-15,997, 1997

Crowley, T., Ice-age methane variations, *Nature, 353*, 122-123, 1991.

Dällenbach, A., T. Blunier, J. Flückiger, B. Stauffer, J. Chappellaz, and D. Raynaud, Changes in the atmospheric CH_4 gradient between Greenland and Antarctica during the Last Glacial and transition to the Holocene, *Geophys. Res. Lett.*, in press, 2000.

Etheridge, D.M., G.I. Pearman, and P.J. Fraser, Changes in tropospheric methane between 1841 and 1978 from a high accumulation rate Antarctic ice core, *Tellus*, Ser. B, *44B*, 282-294, 1992.

Fuchs, A., J. Schwander, and B. Stauffer, A new ice mill allows precise concentration determination of methane and most probably also other trace gases in the bubble air of very small ice samples, *J. Glaciol., 39*, 199-203, 1993.

Fung, I., J. John, J. Lerner, E. Matthews, M. Prather, L.P. Steele, and P.J. Fraser, Three-dimensional model synthesis of the global methane cycle, *J. Geophys. Res., 96*, 13,033-13,065, 1991.

Gasse, F. and E. V. Van Campo, A 40,000-yr pollen and diatom record from Late Tritrivakely, Madagascar, in the southern Tropics, *Quat. Res., 49*, 299-311, 1998.

Grigg, L.D., and C. Whitlock, Late-glacial vegetation and climate change in western Oregon, *Quat. Res., 49*, 287-298, 1998.

Grimm, E. C., G. L. Jacobsen, W.A. Watts, B.C.S. Hansen, and K.A. Maasch, A 50,000 year record of climatic oscillations from Florida and its temporal correlation with the Heinrich events, *Science, 261*, 198-200, 1993.

Grootes, P.M. and E.J. Steig, Taylor Dome ice core study 1993/1994: An ice core to bedrock, *Antarct. J. U. S., 29*, 79-81, 1994.

Grootes, P.M., M. Stuiver, J.W.C. White, S. Johnsen, and J. Jouzel, Comparison of oxygen isotope records from the GISP2 and GRIP Greenland ice cores, *Nature, 366*, 552-554, 1993.

Hein, R., P.J. Crutzen, and M. Heinmann, An inverse modeling approach to investigate the global atmospheric methane cycle, *Global Biogeochem. Cycles, 11*, 43-76, 1997.

Herron, M. M., and C. C. Langway, Firn densification: An empirical model, *J. Glaciol., 25*, 373-385, 1980.

Hughen, K.A., J. T. Overpeck, L.C. Peterson, and S. Trumbore, Rapid climate changes in the tropical Atlantic region during the last deglaciation, *Nature, 380*, 51-54, 1996.

Johnsen, S.J., H. B. Clausen, W. Dansgaard, K. Fuhrer, N. Gundestrup, C. U. Hammer, P. Iverson, J. Jouzel, B. Stauffer, and J. P. Steffensen, Irregular glacial interstadials recorded in new Greenland ice core, *Nature, 359*, 311-313, 1993.

Jouzel, J., et al., Extending the Vostok ice-core record of paleoclimate to the penultimate glacial period, *Nature, 364*, 407-412, 1993.

Kennett, J.P., L.L. Hendy, and R.J. Behl, Late Quaternary foraminiferal carbon isotope record in Santa Barbara Basin: implications for rapid climate change, *EOS, Trans. AGU, 77(46)*, Fall Meeting Supplement, F294, 1996.

Khalil, M.A.K. and R.A. Rassmussen, Atmospheric methane trends over the last 10,000 years, *Atmos. Environ., 21*, 2445-2452, 1987.

Lehman, S., and L. Keigwin, Sudden changes on North Atlantic circulation during the last deglaciation, *Nature, 356*, 757-762, 1992.

Lowe, J., B. Ammann, H. H. Briks, S. Bjorck, G. R. Coope, L. C. Cwynar, J. L. de Beaulieu, R. J. Mott, D. M. Peteet, and M. J. C. Walker, Climatic changes in areas adjacent to the North Atlantic during the last glacial-interglacial transition (14-9 ka); A contribution to IGCP-253, *J. of Quat. Sci., 9*, 185-198, 1994.

Martinerie, P., D. Raynaud, D. M. Etheridge, J.-M. Barnola, and D. Mazaudeir, Physical and climatic parameters which influence the air content of polar ice, *Earth Planet. Sci. Lett., 112*, 1-13, 1992.

Meese, D., R. Alley, T. Gow, P. Grootes, P. Mayewski, M. Ram, K. Taylor, E. Waddington, and G. Zielinski, Preliminary depth-age scale of the GISP2 ice core, *CRREL Spec. Rep. 94-1*, Cold Reg. Res. and Eng. Lab., Hanover, N. H., 1994.

Nakazawa, T., T. Machida, M. Tanaka, Y. Fujii, S. Aoki, and O. Watanabe, Differences of the atmospheric CH_4 concentration between the Arctic and the Antarctic regions in pre-industrial/pre-agricultural era, *Geophys. Res. Lett., 20*, 943-946, 1993.

Nisbet, E.G., Sources of atmospheric methane in early postglacial time, *J. Geophys. Res.*, 97, 12,859-12867, 1992.

Peltier, R., Ice age paleotopography, *Science, 265*, 195-201, 1994.

Petit, J. R., et al., Climate and atmospheric history of the past 420,000 years from the Vostok ice core, Antarctica, *Nature, 399*, 429-436, 1999.

Petit-Maire, N., M. Fontugne, and C. Rouland, Atmospheric methane ratio and environmental changes in the Sahara and Sahel during the last 130 kyrs, *Palaeogeogr., Palaeoclimatol., and Palaeocol., 86*, 197-204, 1991.

Prentice, I.C., Vegetation responses to past climatic variation, *Vegetatio, 67*, 131-141, 1986.

Prinn, R.G., R.F. Weiss, B.R. Miller, J. Huang, F.N. Alyea, D.M. Cunnold, P.J. Fraser, D.E. Hartley, and P.G. Symonds, Atmospheric trends and lifetime of CH_3CCl_3 and global OH concentrations, *Science, 269*, 187-192, 1995

Rasmussen, R. A., and M.A.K. Khalil, Atmospheric methane in the recent and ancient atmospheres: concentrations, trends, and interhemispheric gradient, *J. Geophys. Res., 89*, 11,599-11,605, 1984.

Raynaud, D., J. Chappellaz, J.M. Barnola, Y.S. Korotkevich, and C. Lorius, Climatic and methane cycle implications of glacial-interglacial methane change in the Vostok ice core, *Nature, 333*, 655-657, 1988.

Ritchie, J.C., L.C. Cwynar, and R.W. Spear, Evidence from north-west Canada for an early Holocene Milankovitch thermal maximum, *Nature, 305*, 326-328, 1983.

Sachs, J. P. and S. J. Lehman, Subtropical North Atlantic temperatures 60,000 to 30,000 years ago, *Science, 286*, 756-759, 1999.

Schlesinger, W.H., *Biogeochemistry: an analysis of global change*, 588 pp., Academic, San Diego, Calif., 1996.

Schwander, J., J.-M. Barnola, C. Andrié, M. Leunberger, A. Ludin, D. Raynaud, and B. Stauffer, The age of the air in the firn and the ice at Summit, Greenland, *J. Geophys. Res., 98*, 2831-2838, 1993.

Schwander, J., T. Sowers, J.-M. Barnola, T. Blunier, A. Fuchs, and B. Malaize, Age scale of the air in the summit ice: implication for glacial-interglacial temperature change, *J. Geophys. Res., 102*, 19,483-19,493, 1997.

Severinghaus, J. and E. Brook, Abrupt climate change at the end of the last glacial period inferred from trapped air in polar ice, *Science, 286*, 930-934, 1999.

Severinghaus, J.P., T. Sowers, E.J. Brook, R.B. Alley, and M.L. Bender, Timing of abrupt climate change at the end of the Younger Dryas interval from thermally fractionated gases in polar ice, *Nature, 391*, 141-146, 1998.

Sowers, T., et al., An interlaboratory comparison of techniques for extracting and analyzing trapped gases in ice cores, *J. Geophys. Res., 102*, 26,527-26,538, 1997.

Stauffer, B., E. Lochbronner, H. Oeschger, and J. Schwander, Methane concentration in the glacial atmosphere was only half that of the preindustrial Holocene, *Nature, 332*, 812-814, 1988.

Steig, E.J., Beryllium-10 in the Taylor Dome ice core: applications to Antarctic glaciology and paleoclimatology, Ph.D. thesis, Univ. of Wash., Seattle, 1996.

Steig, E.J., E.J. Brook, J.W.C. White, C. Sucher, S.J. Lehman, M.L. Bender, D.L. Morse, and E.D. Waddington, Synchronous climate changes in Antarctica and the North Atlantic during the last glacial-interglacial transition, *Science, 282*, 92-95, 1998.

Steig, E.J., D.L. Morse, E.D. Waddington, M. Stuiver, P.M. Grootes, and P.A. Mayewski, Wisconsinian and Holocene climate history from an ice core at Taylor Dome, western Ross Embayment, Antarctica, *Geogr. Ann.*, in press, 2000.

Stuiver, M., P.M. Grootes, and T.F. Braziunas, The GISP2 $\delta^{18}O$ climate record of the past 16,500 years and the role of the sun, ocean and volcanoes, *Quat. Res., 44*, 341-354, 1995.

Sucher, C.M., Atmospheric gases in the Taylor Dome ice core: Implications for East Antarctic climate change, M.S. thesis, Univ. of R.I., Narragansett, 1997.

Thompson, A., The oxidizing capacity of the Earth's atmosphere: Probable past and future changes, *Science, 256*, 1,157-1,165, 1992.

Thorpe, R.B., K.S. Law, S. Bekki, J.A. Pyle, and E.G. Nisbet, Is methane-driven deglaciation consistent with the ice core record?, *J. Geophys. Res., 101*, 28,627-28,635, 1996.

Trudinger, C.M., I.G. Enting, D.M, Etheridge, R.J. Francey, V.A. Levchenko, and L.P. Steele, Modeling air movement and bubble trapping in firn, *J. Geophys. Res., 102*, 6747-6763, 1997.

Webb, T., Is vegetation in equilibrium with climate? How to interpret late Quaternary pollen data, *Vegetatio, 67*, 75-91, 1986.

Whiting, G.J., and J.P. Chanton, Primary production control of methane emission from wetlands, *Nature, 364*, 794-795, 1993.

E. Brook and S. Harder, Department of Geology, Washington State University, Vancouver, WA 98686. (brook@vancouver.wsu.edu)

J. Severinghaus, Scripps Institution of Oceanography, University of California, San Diego, La Jolla, CA 92093.

E. Steig, Department of Earth and Environmental Science, University of Pennsylvania, Philadelphia, PA 19104.

C. Sucher, NOAA Office of Global Programs, 1100 Wayne Avenue, Suite 1210, Silver Spring, MD 20910.

(Received June 1, 1999; revised October 26, 1999;
accepted November 2, 1999.)